

# COMPARISON OF THE IMPACT FORCE ON THE BOTTOMHOLE SURFACE BETWEEN PDC AND ROLLER CONE BITS

Sammy Cristopher Paredes Puelles<sup>1</sup>, Elie Luis Martinez Padilla<sup>2</sup>, Jonatas Emmanuel Borges<sup>3</sup>, Marcos Antonio Souza Lourenço<sup>4</sup>

<sup>1,2</sup> *Department of Mechanical Engineering, Federal University of Uberlândia,  
Uberlândia, 38.400-902, Brazil.*

<sup>1</sup>*crisopher.paredes@ufu.br, <sup>2</sup>epadilla@ufu.br*

<sup>3</sup> *Department of Food Engineering, Federal University of Mato Grosso,  
Barra do Garças, 78.600-000, Brazil.*

*jonatas.borges@ufmt.br*

<sup>4</sup>*Department of Mechanical Engineering, Federal University of Technology - Paraná,  
Cornélio Procópio, 86.300-000, Brazil.*

*mlourenco@utfpr.edu.br*

**Abstract.** In the process of drilling the well, the mud is pumped through the drill string, passing through the drill bit until it reaches the ground, and finally the drilling mud with the particulate material is taken to the surface through the annulus region. The impact of the fluid that leaves the nozzles of the drill bit to the ground, will allow the degradation of the soil and removal of the particulate material. The influence of the rotating drill string on the impact force will be studied through a numerical platform under development based on the Navier-Stokes equations, discretized using the finite volume method using staggered arrangement, with a second order of approximation in space and time. The immersed boundary method is employed, where the fluid is represented by the Eulerian mesh and the geometry by the Lagrangian mesh, which in our case will use two different types of drill bits (Polycrystalline Diamond Cut-PDC and Roller cone) to compare them. The Large Eddy Simulation method was also employed with the dynamic sub-grid scale model, which is associated with describing the turbulence phenomenon. The Reynolds number based on the fluid inlet diameter was 3500.

**Keywords:** Impact force, large eddy simulation, drilling process, PDC bit, Roller cone bit.

## 1 Introduction

The phenomena taking place in the downhole region are very complex. The mud leave the drill ejector nozzles with direction on the ground and the drill string will be formed when rotating, an impact ring on the ground. This phenomenon allow the removal of the particulate material left by the cutting drill. The impact force intensity will depend, among other parameters, on the amount of linear fluid movement, and on the rotation rate of the drill string. The increase in the angular velocity of the drilling column will contribute positively or negatively to the increase in the magnitude of the impact force, as shown in this work. This magnitude is considered an important factor in the rate of penetration [7]. Additionally, both numerical studies and physical experiments have been carried out focusing on understanding the dynamic flow and impact force process main parameters, such as dynamic viscosity, volumetric flow rate, density, rotation and drill nozzles diameter [4]; [10]; [3]. Understanding the influence of geometric and mechanical parameters on the flow will help to reduce costs and on the good planning in the previous or subsequent stages of the drilling project, which can make the project even more viable. There are different types of formations in the terrain, and rocks with different hardness can be found in the drilling process. Also, the erosion caused by the fluid in the terrain will create a weakening of it, depending on the

formation and hardness of the material. The drills presented in this work were designed based on the IADC codes M433 [8] and 617X [11] PDC and Roller cone, whose geometries are totally different, thereby forming complex flow patterns with different eddy structure sizes. The impact force for each type of rotating drill is analyzed.

## 2 Physical Model

The geometry studied in the present fluid flow problem is based on a simplified form of the drilling well process, as shown in Fig. 1. Considering a PDC and Roller Cone drill bit, the Lagrangian meshes are built upon its simplifications, where the mesh elements are of triangular shape, each side measuring approximately 8.8 mm.

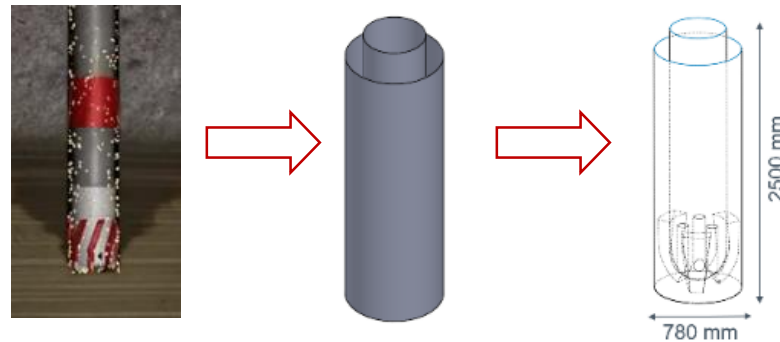


Figure 1. Representation of the problem.

The fluid inlet diameter is 0.5m (500 mm). The drill bit PDC type, whose code according to the IADC is M433, is shown in Fig. 2a. The large diameter is 8 1/2" (215.9 mm) with regular connection API 4 1/2". This corresponds to a drill collar of 5 3/4" (146.05 mm), shown in the Fig. 2a. It was considered only 3 blades and 3 nozzles, which are the sum of volumes of the 6 blades and the sum of the area of the 6 nozzles, respectively, which in theory, would represent the same geometry. The diameter of 8 1/2" was also chosen for the roller cone drill bit (Fig. 2b), corresponding to a Regular API connection of 4 1/2". In the same way that in the previous case, a DC of 5 3/4" will be chosen. In total, it was considered three cones (that's why it will be called a Tricone bit), and three nozzles. After applying the scale factor and having measurements without considering decimal places, the ratio between the diameter of the bit and the duct connecting the bit (DC – Drill Collar) is 1.48.

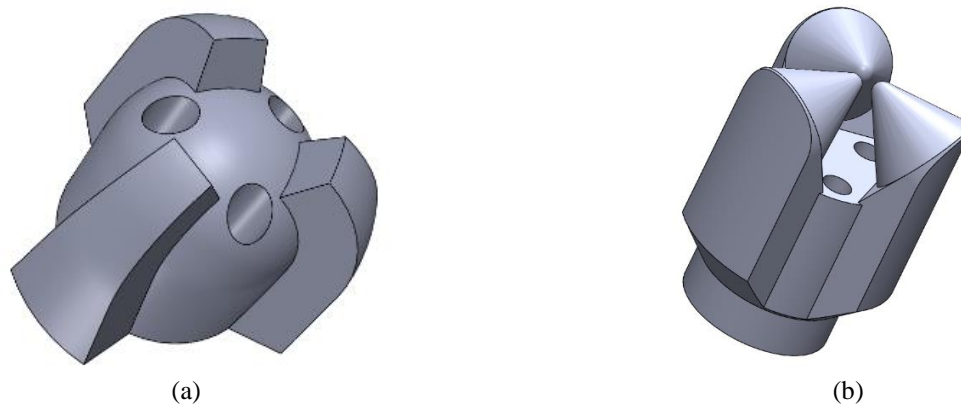


Figure 2. Simplified drill bits used in the drill string. (a) PDC bit (b) Tricone bit.

### 3 Mathematical Model

In order to describe the behavior of the flow, considering Newtonian and incompressible fluid, the model includes the Navier Stokes equations (where the  $I = 1, 2, 3$  and  $j = 1, 2, 3$  index varies by row and column respectively) and the mass conservation equation are, respectively given in Equations 1 and 2 as:

$$\frac{\partial \bar{u}_i}{\partial t} + \frac{\partial (\bar{u}_i \bar{u}_j)}{\partial x_j} = \frac{-1}{\rho} \frac{\partial \bar{p}}{\partial x_i} + \frac{\partial}{\partial x_j} \left[ (\nu + \nu_t) \left( \frac{\partial \bar{u}_i}{\partial x_j} + \frac{\partial \bar{u}_j}{\partial x_i} \right) \right] + \frac{\bar{f}_i}{\rho}, \quad (1)$$

$$\frac{\partial \bar{u}_j}{\partial x_j} = 0, \quad (2)$$

where  $\bar{u}_i$  is the filtered velocity component,  $\bar{p} = \bar{p} + \frac{2}{3} \rho k$  is the modified pressure,  $k$  is the turbulence kinetic energy,  $\rho$  is the specific mass,  $\bar{f}_i$  is the force component, which represents any external force action on the fluid, and  $(\nu + \nu_t)$  is the effective viscosity, that gather both terms of molecular and turbulent viscosities. The Dynamic Sub-Grid Scale model has been used to calculate the turbulent viscosity.

The immersed boundary method (IBM) of direct forcing based model, was used through the addition of source term  $f_i$ , this term is responsible for representing the interface immersed in the Eulerian domain, after passing information to the Lagrangian domain when the term force was solved. It is mathematically written as:

$$\vec{f}(\vec{x}, t) = \int_r \vec{F}(\vec{x}_k, t) \delta(\vec{x} - \vec{x}_k) d\vec{x}_k, \quad (3)$$

where  $\delta(x)$  is the auxiliary Dirac delta function,  $k$  denotes a Lagrangian variable and  $\vec{F}(\vec{x}_k, t)$  is the Lagrangian force, which is determined on the points of the object (physic model) and  $\vec{f}(\vec{x}, t)$  is the Eulerian force.

### 4 Numerical Model

The method of discretization used is the finite volume method, where the velocity variables are on the faces and the pressure variable in the center of the control volume, also known as the staggered arrangement. For the coupling of the pressure and velocity, the method of fractional steps [5] was used. This method consists of two steps, a predictor and corrector steps.

Predictor step:

$$\frac{u_i - u_i^t}{\Delta t} = \frac{2}{3} (-A_i + D_i + f_i)^t - \frac{1}{2} (-A_i + D_i + f_i)^{t-1} - \frac{1}{\rho} \nabla P_i^t, \quad (4)$$

Corrector step:

$$\frac{u_i^{t+1} - u_i}{\Delta t} = \frac{-1}{\rho} \nabla P_i'. \quad (5)$$

where  $P_i' = P_i^{t+1} - P_i^t$ , is the pressure fluctuation and  $A_i$  is the net flow of linear momentum by advection,  $D_i$  is the net flow of linear momentum by diffusion,  $f_i$  is the source term represented by Lagrangian force.

For the direct forcing method, the interpolation and distribution of values between the Eulerian and Lagrangian meshes are done using a reconstruction by moving least square method (MLS).

### 5 Results

In the well-column system (bottomhole) as an input condition, a velocity profile developed for the turbulent regime was employed. In the drill string (which includes the drill bit) rotation speeds of 25, 50, 75 and 100 rpm were considered.

As an output condition, the Neumann condition was used.

The Eulerian mesh of 86x86x286 volumes in the x, y z directions, the Lagrangian mesh used has a ratio of  $ds/dx = 0.88$ . A gap between the bit and the bottomhole surface of 20 mm was considered. The same clearance

value was considered between the maximum bit diameter and the well diameter. The fluid enters the drill string, and passes through all the assembled ducts until it reaches the drill bit where finally the fluid is ejected by the drill nozzles, the drill string is moving counterclockwise (Fig. 3). A quarter of the well (in the angular direction) was not considered for better visualization of the structures formed by the influence of the column rotation and the axial movement with direction in the annular part of the system.

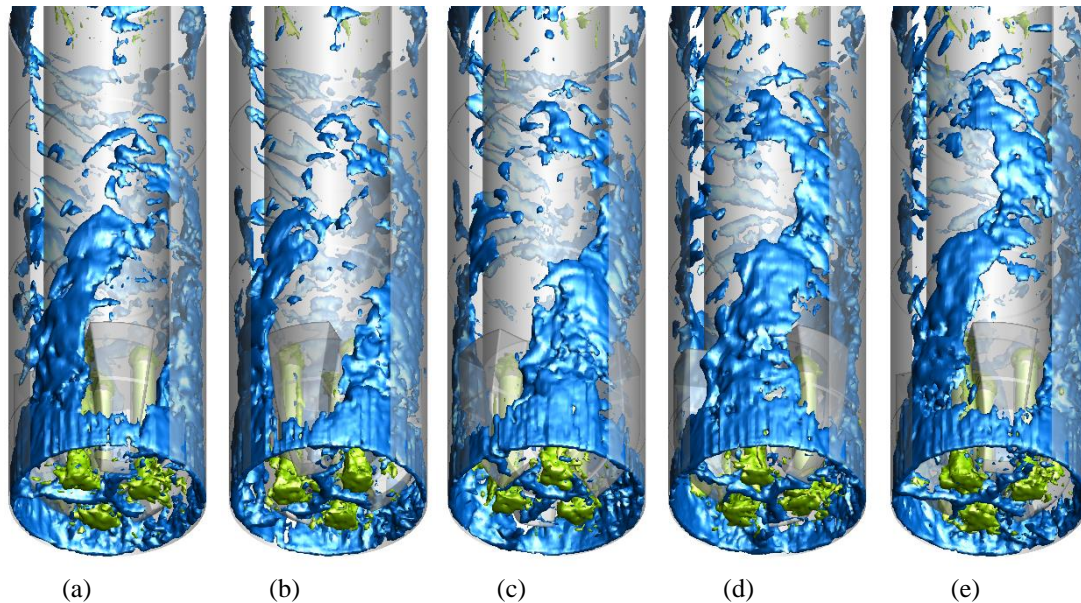


Figure 3. Temporal evolution of the flow represented by so-surfaces  $w=0.45\text{m/s}$  (green) e  $w= -0.34\text{m/s}$  (blue); for 25 rpm and time: (a)  $t=3.8\text{s}$  (b)  $t=4.0\text{s}$  (c)  $4.2\text{s}$  (d)  $4.4\text{s}$  (e)  $4.6\text{s}$ .

In order to observe the structures of the turbulent regime within the domain, the Q criterion is used, using iso-surfaces with a value of 300 (1/s) colored by the velocity module (Fig.4). The eddy structures typical of turbulent flows are present in various sizes, basically in the form of filaments. For low rotation speeds of the drill string, these structures are concentrated around the drill bit, increasing the rotation speed generates a multiplier effect until filling the annular duct.

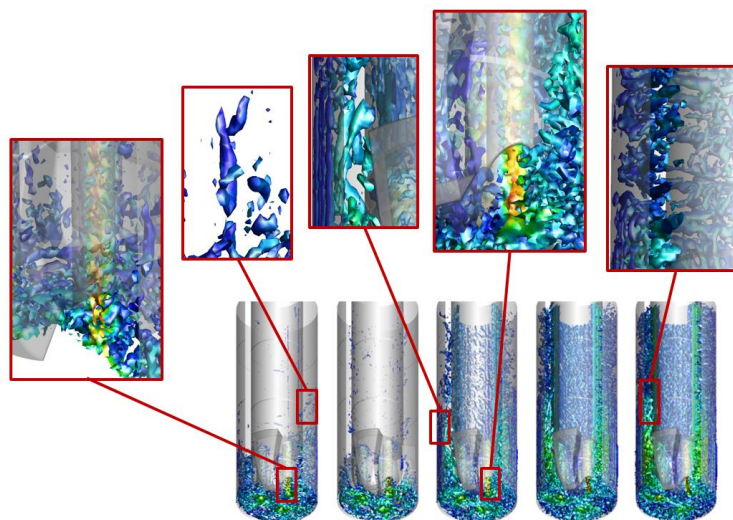


Figure 4. Representation of eddy structures using the Q criterion; PDC; (a) 0 rpm, (b) 25 rpm, (c) 50 rpm, (d) 75 rpm, (e) 100 rpm.

The dynamics of the flows has a direct influence on the static pressure exerted on the bottomhole surface, and this characteristic is fundamental to determine the operational parameter of great interest in drilling projects, the impact force. Certainly, the drill geometry and the column rotation speed influence this parameter [1]; [2]; [6]. In Fig. 5 shows the bottomhole surface pressure field for the PDC drill bit as a consequence of the impact of the jets on the



surface and the amount of linear motion applied by the return flow. By the balance of linear momentum, at the bottom of the well there is an increase in the static pressure of the fluid, however there is a drop in energy corresponding to the total pressure. For the case without rotation, a slight increase is recorded (Fig. 5a), and two regions of concentric circumferences for the cases with rotation (Fig. 5b-c). This pattern is repeated for the tricone bit configuration (Fig. 6), differing mainly in magnitude, which on average is higher for the tricone bit [9].

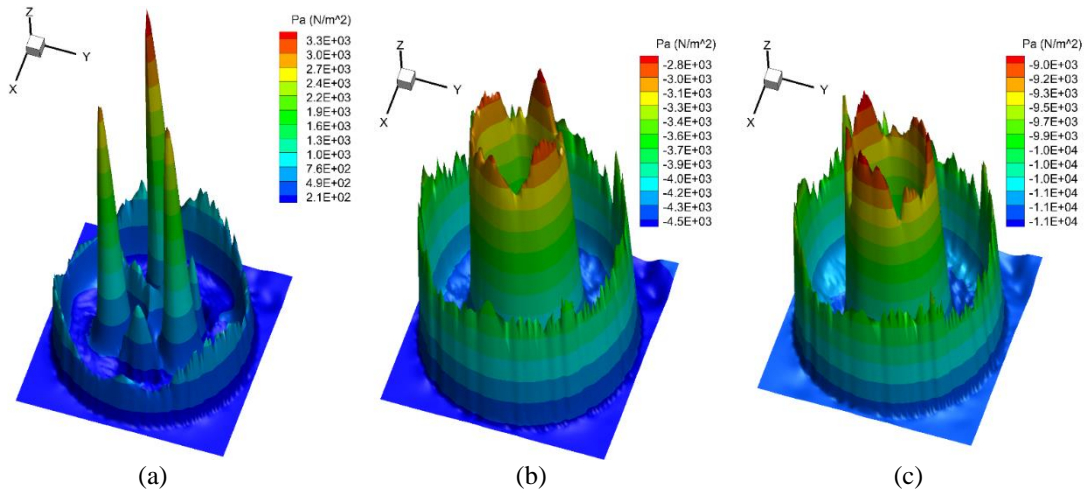


Figure 5. PDC bit. Magnitude of the average bottomhole pressure, for rotations: (a) 0 rpm, (b) 25 rpm (c) 50 rpm

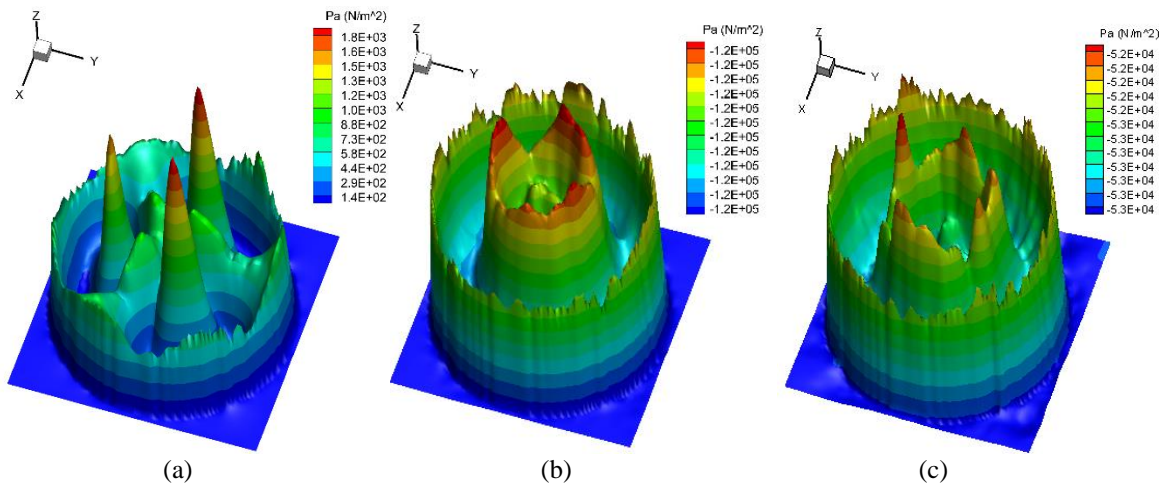


Figure 6. – Tricone bit. Magnitude of the average bottomhole pressure, for rotations: (a) 0 rpm, (b) 25 rpm (c) 50 rpm

Table 1. –Mean values of impact force for PDC and Tricone drill bit, influenced by rotation

RPM	Bit	
	PDC F (N)	Tricone F (N)
0	160.477	333.329
25	463.184	733.861
50	443.955	573.192
75	351.578	531.397
100	362.665	603.003

In the present proposal, the impact force will be obtained by the immersed boundary method, through the quantification of the Lagrangian force. The average values of the impact force are presented in Tab. 1, corresponds to the time signals. The highest impact force corresponds to the tricone bit, oscillating between 129 and 240 N of difference compared to the values of the PDC bit.

The oscillations increase with the rate of rotation, giving rise to high intensity product peaks. Such signals in average values are shown in Fig. 7, which explains the impact force as a function of the rotation rate. It is noticed that the trend of the curves formed by the points of impact force for the PDC and Tricone drill types are not parabolic, but follow the same pattern. That is, the rotation speed increases the impact force up to approximately 25 rpm, a value from which it decreases. It is also confirmed, as indicated by the pressure fields, that with the tricone bit, the impact force is greater than with the PDC type (for the case of simplified bits in this specific problem).

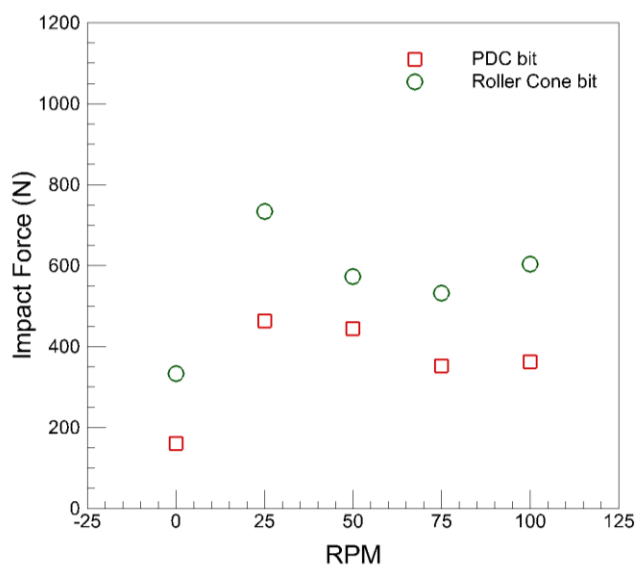


Figure 7. Impact force influenced by the rotation of the proposed drills

## 6 Conclusions

In the bottomhole region, different structures were found, product of rotation and flow ejection. High values of static pressure magnitude were found on the bottomhole surface, evidenced by the three-dimensional pressure fields, such fields, have a ring shape by the rotation effect.

The effect of drill string rotation directly influences the magnitude of the impact force on the bottomhole. The curves formed by the values of the impact force as a function of the RPM of both configurations of drills, are not parabolic, presenting an increase up to 25 rpm, after this value, the values decrease with a tendency to rise again.

**Acknowledgements.** The authors wish to thank the Petrobras, FAPEMIG, CAPES, Federal University of Uberlândia (UFU), FEMEC.

**Authorship statement.** The authors hereby confirm that they are the sole liable persons responsible for the authorship of this work, and that all material that has been herein included as part of the present paper is either the property (and authorship) of the authors, or has the permission of the owners to be included here.

## References

- [1] Borges, J. E. Modelagem e simulação numérica de escoamentos simplificados no fundo de poços em perfuração. Tese do Doutorado. Universidade Federal de Uberlândia, Uberlândia, Brasil. 2020.
- [2] Borges, J. E. Large-eddy simulation of downhole flow: the effects of flow and rotation rates. University of Uberlândia, Minas Gerais, Brazil. (2020).
- [3] Daroz, V.; Maneira, E. L.; Franco, A. t. Investigação numérica da circulação direta e reversa no processo de perfuração de poços de petróleo. VI Encontro Nacional de Hidráulica de Poços de Petróleo e Gás, 2015.
- [4] Figueiredo, L. M.; Neves, D. S. das; Silva, L. C.; Franco, A. T.; AO, C. O. R. N.; Morales, R. E. M.; Waldman, A. T.; Martins, A. L. Investigação da força de impacto e do coeficiente de descarga em bocais ejetores de brocas de perfuração. V Encontro Nacional de Hidráulica de Poços de Petróleo e Gás, 2013.
- [5] Kim, J.; Moin, P. Application of Fractional-Step Method to Incompressible Navier-Stokes Equations. ScienceDirect, California, p. 308-323, 4 September 1984. [https://doi.org/10.1016/0021-9991\(85\)90148-2](https://doi.org/10.1016/0021-9991(85)90148-2)
- [6] Maneira, E. L. Estudo da hidráulica de brocas de perfuração de poços – efeitos de parâmetros do processo de perfuração. 2013. Monográfica (Engenharia Mecânica), Universidade Tecnológica Federal do Paraná, Curitiba, Brasil.
- [7] Micon-Drilling, G. Catálogo. 2016. P. 43. Drilling equipment Made in Germany.
- [8] Figueiredo, L. M. Investigação numérica da força de impacto e do coeficiente de descarga em bocais ejetores de brocas perfuração. Universidade Tecnológica Federal do Paraná. Curitiba. 2014.
- [9] Puelles, S. C. P., Aplicação do método de fronteira imersa no estudo de escoamentos no fundo de poço, considerando brocas simplificadas. Dissertação de Mestrado, Universidade Federal de Uberlândia, Brasil. 2019.
- [10] Santos, V. T. S. Estudo experimental da força de impacto e do coeficiente de descarga de bocais ejetores utilizados na perfuração de poços de petróleo. 2014. Monografia (Engenharia Mecânica), Universidade Tecnológica Federal do Paraná, Curitiba, Brasil.
- [11] SMITH, B. P. Schlumberger, 2018. Disponível em: <[https://www.slb.com/~media/Files/smith/catalogs/bits\\_catalog.pdf](https://www.slb.com/~media/Files/smith/catalogs/bits_catalog.pdf)>. Acesso em: 25 Abril 2019.